Transfer versus compound-nuclear mechanism in the reaction of ^{12}C and ^{11}B with ^{63}Cu and ^{65}Cu†

Robert A. Williams* and Albert A. Caretto, Jr.
Carnegie-Mellon University, Pittsburgh, Pennsylvania 15213
(Received 4 February 1974)

Excitation functions and average projected ranges have been measured for the production of ^{66}Ga and ^{70}As from enriched ^{63}Cu and ^{65}Cu targets with ^{11}B and ^{12}C projectiles of 10.5 MeV/amu. In addition, angular and range distributions were determined for the same products from ^{63}Cu and ^{65}Cu with 90 MeV ^{12}C ions. The results are compared with predictions based on the complete fusion compound nucleus mechanism and a quasielastic scattering model designed to represent transfer mechanisms. The results indicate that a number of the reactions must take place by more than one pathway.

[NUCLEAR REACTIONS $^{65,63}Cu(^{11}B, X)^{66}Ga$, $^{65,63}Cu(^{12}C, X)^{70}As$, separated isotope targets, $E = 23-117$ MeV; measured $\sigma(E)$, recoil fragment (E), and fragment $\sigma(E, \theta)$ for 90 MeV ^{12}C.]

INTRODUCTION

Recent studies[1-4] of heavy ion reactions have shed new light on the role of transfer reactions. Their most significant impact has been nearly to dissolve the clear experimental distinction between transfer and complete fusion compound nucleus (CFCN) mechanisms for some reaction products. The early qualitative model of Kaufman and Wolfgang[5,6] has been largely substantiated and extended to describe the transfer of masses comparable to that of the projectile. Thus far, most of the research reported has involved the measurement of the lighter fragments ejected from such reactions. This work investigates the use of the somewhat more restrictive radiochemical measurements of the heavy residues as a means for distinguishing between transfer and CFCN mechanisms. Product excitation functions, angular, and range distributions were determined in order to indicate the probability of the various reaction paths.

EXPERIMENTAL PROCEDURE

Self-supporting ^{63}Cu and ^{65}Cu targets of 2–3 mg/cm^2 thickness and enriched to 99.73 and 99.70%, respectively, were prepared by an electrodeposition technique described in detail elsewhere.[7] These were used in the measurement of excitation functions and average ranges. Thinner (~300 μg/cm^2) targets, electrodeposited via a similar technique onto backings of thin carbon sheet, were used in the determination of angular and range distributions. ^{12}C and ^{11}B beams, with a maximum energy of 10.5 MeV/amu, were provided by the heavy ion linear accelerator at Yale University. Average currents were approximately 80 nA for ^{11}B and 120 nA for ^{12}C (1.2 and 1.5×10^{11} heavy ions per sec, respectively). Collimation reduced the beam intensities for the angular and range distributions well below these values.

Excitation functions and average (projected) ranges were ascertained simultaneously by the stacked foil method, with aluminum foils of varying thicknesses used both as recoil catchers and as beam energy degraders. No catcher was less than 2.5 mg/cm^2 thick. The beam energy at any point in the stack was determined by a two-dimensional interpolation in Northcliffe's tables.[8] (These tables were used for all range-energy conversions throughout this work.) The range distribution measurements employed a stack of aluminum leaf foils (~160 μg/cm^2 each) mounted on 3 mil aluminum annuli. Each foil corresponded to about 7% of the maximum range observed. The apparatus for the angular distributions utilizes a flat catcher foil mounted perpendicular to the heavy ion beam and has been described in detail elsewhere.[9,10] For these experiments, the catcher foil was mounted close enough to the target to result in a maximum observable recoil angle of about 54°. After irradiation the catcher foil was cut into concentric rings for product analysis. Each annulus thus obtained corresponds to an exactly known range of recoil angles.

The activity of each sample was determined, without performing chemical separation, by use of a large-volume, high resolution Ge(Li) detector at Yale. All γ spectra were analyzed by the BRUTAL computer program[11] which involved a search of the entire spectrum for peaks, the identification of doublet and triplet peaks, and the integration of each peak which was significantly above background. A decay curve least squares

fit of the integrated γ activities was obtained by use of the CLSQ computer program. This yielded end-of-bombardment activities from which all cross sections were calculated.

RESULTS

Excitation functions for eight different reactions were determined; specifically, those involving the production of ^{66}Ga and ^{70}As from ^{63}Cu and ^{65}Cu separated isotope targets from the interaction with ^{11}B and ^{12}C projectiles. These excitation functions are presented in Figs. 1 and 2. The open circles with arrows in these figures represent a lack of measurable activity for that energy and are plotted at a height of either 1 mb or the estimated upper limit, whichever is greater.

Figure 3 shows the variation of average projected range in copper with energy for some of these reactions. The solid lines in this figure are the ranges that would result by assuming that the reaction takes place via a CFCN mechanism, i.e., that the product range is primarily a result of the center of mass motion. For simplicity it is also assumed that subsequent particle evaporation has a negligible effect on the range. For α particle emission, however, deviations from the predicted CFCN ranges might be anticipated.

In addition to the experimental angular distributions for all four ^{12}C reactions, Fig. 4 displays the results of a Monte Carlo computer simulation (by a program named EVAP[12]) of the evaporation of particles ($n, p, d, t,$ ^{3}He, or ^{4}He) from a completely fused system of target and projectile at the proper excitation energy (75.3 MeV for ^{75}Br and 74.8 MeV for ^{77}Br). At each step in the evaporation the perturbation on the excited nucleus' original momentum and angle caused by the emitted particle was noted so that the final angular distribution of a given product could be determined. The ordinate of these calculated angular distributions was adjusted such that the calculated peak height was approximately the same as the experimental angular distribution peak height. The $^{12}C + {}^{65}Cu \rightarrow {}^{66}Ga + X$ system is lacking the theoretical histogram because the ^{77}Br excitation energy was insufficient to produce any ^{66}Ga residue nuclei out of 1500 nuclei "evaporated." These angular distributions and the range distributions described below were measured only at a projectile energy of approximately 90 MeV.

The range distributions in aluminum for these

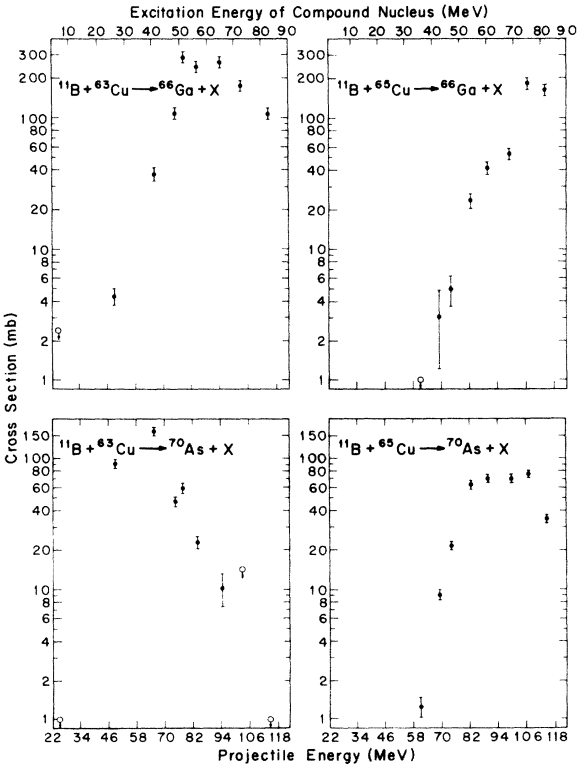

FIG. 1. Excitation functions for the production of ^{66}Ga and ^{70}As from the reaction of ^{11}B with the separated isotopes of Cu. The excitation energy resulting from the production of the compound nucleus is indicated by the top scale.

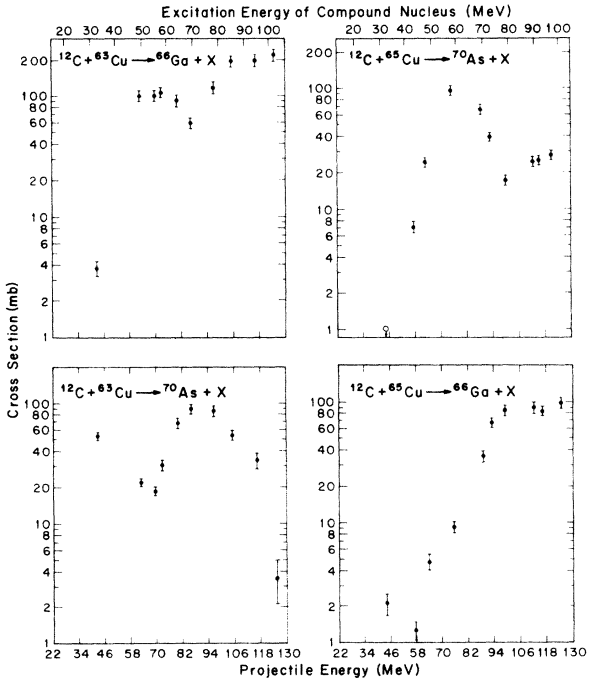

FIG. 2. Excitation functions for the production of ^{66}Ga and ^{70}As from the reaction of ^{12}C with the separated isotopes of Cu. The excitation energy resulting from the production of the compound nucleus is indicated by the top scale.

^{12}C reactions are displayed in Fig. 5. These data were arbitrarily fitted (by a weighted least squares procedure) with single or double Gaussian forms. The result of these fits are superimposed on the experimental histograms and, for the double Gaussians, the relative areas of each component are given. Asterisks appearing in the angular and range distributions indicate that that sample was not counted soon enough to ascertain the intensity of the ^{70}As component. The target thickness employed (~300 $\mu g/cm^2$) causes a broadening of the distribution but does not appreciably affect the peak position.[13]

The uncertainties in these data arise entirely from the known or estimated probable errors of each parameter involved in the calculations, combined according to the appropriate relations.[7] The major contributor to these uncertainties was the random error associated with integration of spectral peaks, but uncertainties in half-life values and branching ratios taken from the literature,

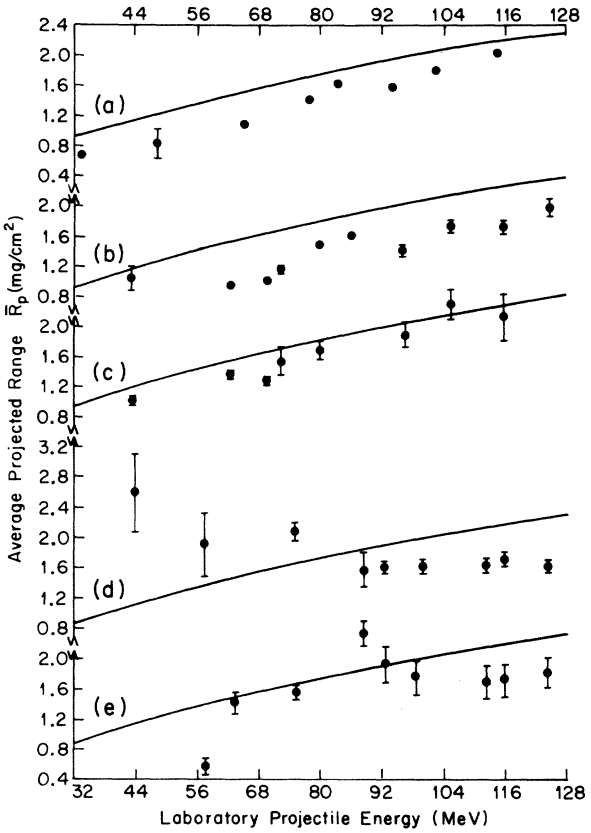

FIG. 3. Variation of average projected range with laboratory projectile energy for five reactions: (a) $^{11}B + {}^{63}Cu \rightarrow {}^{66}Ga + X$, (b) $^{12}C + {}^{63}Cu \rightarrow {}^{66}Ga + X$, (c) $^{12}C + {}^{63}Cu \rightarrow {}^{71}As + X$, (d) $^{12}C + {}^{65}Cu \rightarrow {}^{66}Ga + X$, (e) $^{12}C + {}^{65}Cu \rightarrow {}^{70}As + X$.

beam intensity, and target density were also folded into the computations.

DISCUSSION

There is a striking difference between the excitation functions illustrated in Figs. 1 and 2. The excitation functions initiated by ^{12}C projectiles exhibit multiple peaks which are strong indications of more than one mechanistic pathway, especially when compared to the ^{11}B induced reactions where this behavior is not exhibited. The former set was therefore chosen for primary attention in this study. In consideration of the Q values for the four reactions in Fig. 2, the higher energy peak can most probably be assigned to a process involving fusion of most or all of the projectile with the target followed by multiple particle evaporation. For example, for the reaction $^{63}Cu + {}^{12}C \rightarrow {}^{66}Ga + X$, if X represents four protons and five neutrons the Q value is approximately -71 MeV, while if X represents two α particles and a neutron the Q value is about -15 MeV. In a similar manner for the reaction $^{63}Cu + {}^{12}C \rightarrow {}^{70}As + X$, the Q value is about -40 MeV when X represents individual nucleons, and -12 MeV when a α particle is involved. Thus, the assignment of the CFCN mechanism for the high energy peaks in the excitation functions is consistent with the reaction Q values. Depending on reaction pathway, the low energy peaks may not be consistent with this mechanism.

The average projected range measurements (Fig. 3) are useful in detecting gross changes in the amount of forward momentum given to the products in the reaction. A simple kinematic model representing quasielastic scattering[14] clearly demonstrates the changes in forward momentum which take place as a result of the fusion of less than the full projectile mass with the target. The model first assumes that a portion of the projectile mass is completely absorbed by the target, and this fused system is given a momentum equal to that fraction of the projectile momentum represented by the absorbed part of the projectile. The remainder of the projectile is then assumed to elastically scatter from the fused system, giving the latter an additional recoil momentum. Both steps are described by standard equations of energy and momentum conservation. An example of the results of this calculation for the $^{12}C + {}^{63}Cu$ reaction is illustrated in Fig. 6. The shape of the $^{12}C + {}^{65}Cu \rightarrow {}^{66}Ga + X$ average range curve Fig. 3(d) matches well that for α transfer as predicted by this quasielastic model. The deviation of the ranges illustrated in Fig. 3 from the predicted CFCN range, within the limitations of the experi-

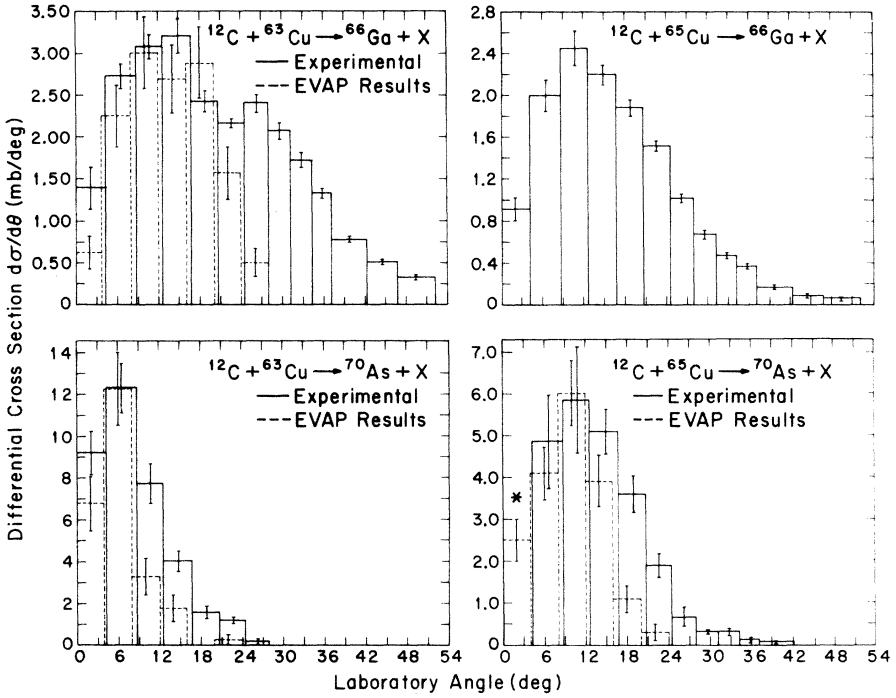

FIG. 4. Variation of differential production cross section with laboratory angle for the four ^{12}C reactions indicated on graphs. Dotted histograms are theoretical predictions resulting from an assumed CFCN mechanism.

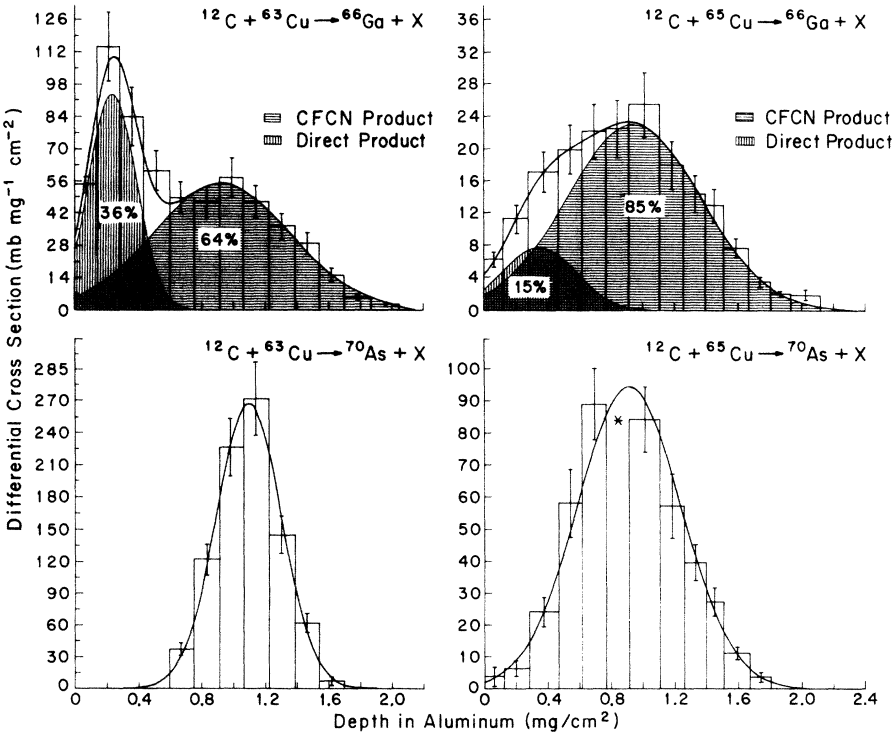

FIG. 5. Variation of differential production cross section with projected recoil fragment kinetic energy for the four ^{12}C reactions indicated on the graphs. The ^{66}Ga product distributions are divided into moieties resulting from CFCN and direct reaction mechanisms.

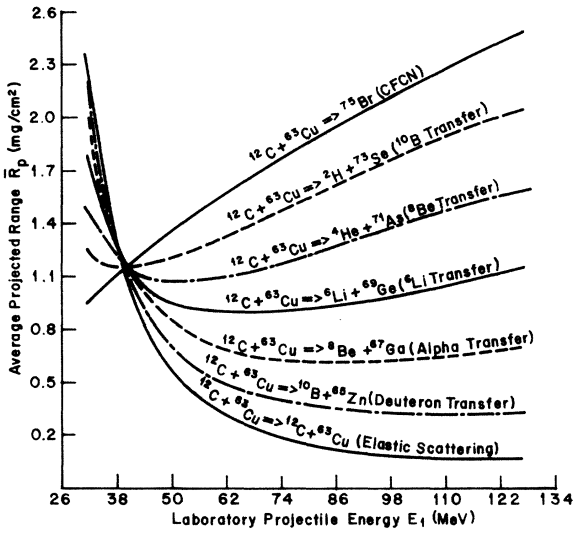

FIG. 6. Average projected range in mg/cm^2 versus laboratory projectile energy for various mass transfers to the target based on the quasielastic scattering model. The $^{12}C + ^{63}Cu$ reaction is illustrated.

mental uncertainties and the neglect of the affect of particle evaporation on range, indicates a degree of admixture of non-CFCN processes which is roughly proportional to the extent of deviation. If this admixture is large enough, the trend of the data will be altered as well, as in Figs. 3(d) and 3(e).

The energies at which the angular and range distributions were done encompasses a wide range of conditions in the four reactions as can be seen by an examination of Fig. 2. Where 90 MeV falls at a minimum in the excitation function, e.g. in the $^{12}C + ^{63}Cu \rightarrow ^{66}Ga + X$ reaction, two components are observed in the angular and range distributions; however, in other reactions, when it is near a maximum in the excitation function, simple angular and range distributions result. These considerations are important in assigning mechanisms to the reactions.

Of equal value are predictions calculated from treating the reaction as if it takes place by the CFCN mechanism. The evaporation calculation results included in Fig. 4 are such predictions. Within the limitation of the statistics based on 1500 evaporations from ^{77}Br at 75.3 MeV excitation energy, the failure of the calculation to predict the production of any ^{66}Ga, resulting from the interaction of ^{12}C with ^{65}Cu, implies that there is probably a negligible CFCN contribution in this case. The somewhat larger peak angle of the theoretical distribution in the $^{12}C + ^{63}Cu \rightarrow ^{66}Ga + X$ reaction, as compared with the $^{12}C + ^{63}Cu \rightarrow ^{70}As + X$ reaction, arises from the sole evaporation mode at this energy (as predicted by the evaporation calculations) of two α particles and a neutron, causing a less forward peaked reaction product than if there had been only single nucleon emissions. The agreement of the evaporation predictions with the low-angle part of the angular distributions, as well as the wide separation of peaks in the angular and range distributions provides support for the assignment of the reaction mechanisms.

In view of the previous discussion, the notation, CFCN product, in Fig. 5 for the $^{12}C + ^{65}Cu \rightarrow ^{66}Ga + X$ reaction may be misleading. Alternative reaction paths and or mechanisms other than CFCN may play an important role in this reaction. The lack of "peak" separation in Figs. 4 and 5 is consistent with this suggestion. One alternative might be ^{8}Be transfer, which is consistent with the work of Bimbot, Gardes, and Rivet.[3] It requires the subsequent evaporation of one α particle and three neutrons (or the equivalent) causing a broad range distribution like the one shown in Fig. 5 for the major component of this reaction.

The experimental results for the production of ^{70}As can also be compared with the predictions based on the evaporation calculation results. The reasonable agreement in the peak angle predictions for both reactions, despite the significant difference in the angle observed for the ^{63}Cu and ^{65}Cu targets, is support of a CFCN interpretation of the reaction mechanism. Furthermore, the evaporation calculations provide an explanation for the peak angle difference in that a predominance of single nucleon emissions from the $^{12}C + ^{63}Cu$ compound nucleus was observed compared with the absence of any mode other than one-α-three-neutron evaporation observed from the ^{77}Br fused system. This implies that both reactions proceed primarily by CFCN mechanisms. The range distributions, however, are not completely consistent with this interpretation. While the peak of the ^{70}As range distribution from the $^{12}C + ^{63}Cu$ reaction falls at 1.09 mg/cm^2 (12.6 MeV), see Fig. 5, and agrees well with the predicted CFCN recoil energy (13.2 MeV), the other ^{70}As peak falls at 0.91 mg/cm^2, a range corresponding to a recoil kinetic energy a full 2.8 MeV below the CFCN predicted range of 12.6 MeV. This discrepancy might result, at least partly, from the assumption that α evaporation does not affect the CFCN ranges predicted solely on the basis of center of mass motion. However, the location of 90 MeV in the excitation function, Fig. 2, well below the higher-energy peak suggests that this product does not result exclusively by the CFCN mechanism.

Consistent but not necessarily conclusive sup-

TABLE I. Kinematic plausibility of various reaction pathways.

Reactants	Reaction Products	Observed nuclide	Q [a] (MeV)	E_R (MeV)	φ (deg)	E^* (MeV)
$^{12}C+^{63}Cu$	$^{66}Ga+^{9}Be$	^{66}Ga	−13.227	1.60	25	13.4
	$^{67}Ga+^{8}Be$	^{66}Ga	−3.662	1.60	25	15.8
	$^{68}Ga+^{7}Be$	^{66}Ga	−14.278	1.60	25	<0
$^{12}C+^{65}Cu$	$^{66}Ga+^{11}Be$	^{66}Ga	−22.058	2.48	24	23.5
	$^{67}Ga+^{10}Be$	^{66}Ga	−11.325	2.48	24	30.5
	$^{68}Ga+^{9}Be$	^{66}Ga	−9.859	2.48	24	27.4
	$^{69}Ga+^{8}Be$	^{66}Ga	−1.201	2.48	24	30.3
	$^{70}Ga+^{7}Be$	^{66}Ga	−12.455	2.48	24	11.7
$^{12}C+^{63}Cu$	$^{70}As+^{5}He$	^{70}As	−12.715	12.36	6	59.7
	$^{71}As+^{4}He$	^{70}As	−0.114	12.36	6	71.6
	$^{72}As+^{3}He$	^{70}As	−12.295	12.36	6	58.1
$^{12}C+^{65}Cu$	$^{71}As+^{6}He$	^{70}As	−15.288	9.24	12	50.4
	$^{72}As+^{5}He$	^{70}As	−8.818	9.24	12	54.6
	$^{73}As+^{4}He$	^{70}As	+2.914	9.24	12	62.8
	$^{74}As+^{3}He$	^{70}As	−9.659	9.24	12	44.3

[a] Computed from the 1964 Atomic Mass Table of Mattauch, Thield, and Wapstra (Ref. 15).

port for the proposed reaction mechanisms can be ascertained by calculating the excitation energy available resulting from various transfers to the target. The standard conservation equations are applied:

$$E_i = E_L + E_R + E^* - Q,$$

$$P_i = P_L \cos\theta + P_R \cos\varphi,$$

$$P_L \sin\theta = P_R \sin\varphi,$$

where the subscript i refers to the incident particle, L the light reaction product, and R the heavy recoil product. These can be easily solved for E^*, the excitation energy of the residual system, in terms of the experimentally determined parameters E_R and φ obtained from the 90 MeV incident energy experiments. The Q value is determined by assuming a specific pathway for the reaction. If, for instance, we assume that an α particle is transferred from ^{12}C to ^{63}Cu, then the ^{67}Ga residue must have an E^* consistent with the evaporation of one and only one neutron, about 8–10 MeV. If the resulting excitation energy is too low, then the reaction as depicted is disallowed; if too high the reaction as depicted may still take place since some of the excitation energy may be associated with the light product. The results of these computations for several hypothetical pathways are given in Table I. This method is particularly well suited to the study of transfer reactions in which only neutrons need to be evaporated from a direct transfer product in order to obtain the observed nuclide. All of the trial cases considered in Table I are examples of this type of mechanism. The number of neutrons which need to be evaporated determines the allowable range of excitation energies E^*. The table shows that ^{66}Ga production via ^{5}He transfer (^{7}Be residual light nucleus) to either ^{63}Cu or ^{65}Cu is energetically disallowed because of insufficient excitation energy. While either ^{4}He or ^{3}He transfer is consistent with the observed angles and energies, the former is more probable, since we are dealing with a projectile which has a definite α structure. α particle transfer, therefore, is expected to be the dominant transfer mode in the $^{12}C+^{65}Cu \rightarrow {}^{66}Ga+X$ system also, even though the present analysis shows ^{3}He transfer and two-proton transfer to be about as consistent with the observed quantities. Note that none of the trial paths for the formation of ^{70}As from $^{12}C+^{63}Cu$ are energetically plausible. This result is in agreement with previously mentioned indications that this is a CFCN product. ^{70}As production from ^{65}Cu, however, is shown to be consistent with a ^{9}Be-transfer mechanism. Although the E^* resulting from the ^{8}Be-transfer assumption seems too high, the extra energy above that necessary for neutron evaporation may be taken up by ^{4}He excitation. (Note that this is the only pathway for which the Q value is positive.)

TABLE II. Postulated reaction mechanisms at 90 MeV.

Reactants	Observed nuclide	Method(s) of production
$^{12}C+^{63}Cu$	^{66}Ga	CFCN + α transfer
	^{70}As	CFCN
$^{12}C+^{65}Cu$	^{66}Ga	^{8}Be transfer + α transfer [a]
	^{70}As	^{8}Be transfer [b]

[a] The α-transfer mode appears to play a minor role here.

[b] CFCN may also be responsible for the production of this nuclide.

All of the above considerations are summarized in Table II. The results presented here clearly indicate that the CFCN mechanism is not solely responsible for all the reactions studied. Various types of transfer processes are the most likely contributors.

ACKNOWLEDGMENTS

The authors wish to express their gratitude to Barclay Jones and the operating crew of the Yale heavy-ion linear accelerator for their invaluable assistance during the bombardments, to Dr. M. Weisfield for his aid and advice in carrying out the experiments, and to Dr. John A. Urbon for running and obtaining the results from the computer program EVAP.

†Work supported by the United States Atomic Energy Commission.

*Present address: Los Alamos Scientific Laboratory, Los Alamos, New Mexico 87544.

[1]J. Galin, D. Guerreau, M. Lefort, J. Peter, X. Tarrago, and R. Basile, Nucl. Phys. A159, 461 (1970).

[2]J. Galin, D. Guerreau, M. Lefort, and X. Tarrago, J. Phys. (Paris) 32, 7 (1971).

[3]R. Bimbot, D. Gardes, and M. F. Rivet, R. C. 72-01, Lab de Chimie Nucleaire, Institut de Physique Nucleaire, B.P.1, Orsay, France.

[4]R. Bimbot, D. Gardes, and M. F. Rivet, Phys. Rev. C 4, 2180 (1971).

[5]R. Kaufman and R. Wolfgang, Phys. Rev. 121, B192 (1961).

[6]R. Kaufman and R. Wolfgang, Phys. Rev. 121, 206 (1961).

[7]R. A. Williams, Ph.D. thesis, Carnegie-Mellon University, June, 1972 (unpublished).

[8]L. C. Northcliffe and R. F. Schilling, Nucl. Data A7, 233 (1970).

[9]M. Kaplan and A. Ewart, Phys. Rev. 148, 1123 (1966).

[10]G. N. Simonoff and J. M. Alexander, Phys. Rev. 133, B104 (1964).

[11]R. Gunnink, H. B. Levy, and J. B. Niday, UCID Report No. UCID-15140 (unpublished), as modified by B. R. Erdal.

[12]F. M. Kiely, Ph. D. thesis, Carnegie Institute of Technology, 1967 (unpublished).

[13]M. Kaplan and V. Subrahmanyam, Phys. Rev. 153, 1186 (1967).

[14]P. M. Strudler, I. L. Preiss, and R. Wolfgang, Phys. Rev. 154, 1126 (1967).

[15]J. H. E. Mattauch, W. Thield, and A. H. Wapstra, Nucl. Phys. 67, 1 (1965).